

Self-Supervised Audio-Visual Representation Learning with Relaxed Cross-Modal Synchronicity

Pritam Sarkar^{1,2} Ali Etemad¹

¹ Queen’s University, Canada ² Vector Institute
{pritam.sarkar, ali.etemad}@queensu.ca
<https://pritamqu.github.io/CrissCross>

Abstract

We present **CrissCross**, a self-supervised framework for learning audio-visual representations. A novel notion is introduced in our framework whereby in addition to learning the intra-modal and standard ‘synchronous’ cross-modal relations, CrissCross also learns ‘asynchronous’ cross-modal relationships. We perform in-depth studies showing that by relaxing the temporal synchronicity between the audio and visual modalities, the network learns strong generalized representations useful for a variety of downstream tasks. To pretrain our proposed solution, we use 3 different datasets with varying sizes, Kinetics-Sound, Kinetics400, and AudioSet. The learned representations are evaluated on a number of downstream tasks namely action recognition, sound classification, and action retrieval. Our experiments show that CrissCross either outperforms or achieves performances on par with the current state-of-the-art self-supervised methods on action recognition and action retrieval with UCF101 and HMDB51, as well as sound classification with ESC50 and DCASE. Moreover, CrissCross outperforms fully-supervised pretraining while pretrained on Kinetics-Sound. The codes, pretrained models, and supplementary material are available on the project website.

1 Introduction

In recent years, self-supervised learning has shown great promise in learning strong representations without human-annotated labels (Chen et al. 2020; Chen and He 2021; Caron et al. 2018), and emerged as a strong competitor for fully-supervised pretraining. There are a number of benefits to such methods. Firstly, they reduce the time and resources required for expensive human annotations and allow researchers to directly use large uncurated datasets for learning meaningful representations. Moreover, the models trained in a self-supervised fashion learn more abstract representations, which are useful for a variety of downstream tasks without needing to train the models from scratch. Given the abundance of videos, their spatio-temporal information-rich nature, and the fact that in most cases they contain both audio and visual streams, self-supervised approaches are strong alternatives to fully-supervised methods for video representation learning. Moreover, the high dimensionality

and multi-modal nature of videos make them difficult to annotate, further motivating the use of self-supervision.

The common and standard practice in self-supervised audio-visual representations learning is to learn intra-modal and cross-modal relationships between the audio and visual streams by maintaining tight temporal synchronicity between the two modalities (Alayrac et al. 2020; Korbar, Tran, and Torresani 2018; Alwassel et al. 2020; Asano et al. 2020). Yet, the impact of learning temporally asynchronous cross-modal relationships in the context of self-supervised learning has not been explored. This notion deserves deeper exploration as learning such temporally asynchronous cross-modal relationships may in fact result in increased invariance and distinctiveness in the learned representations.

In this study, in an attempt to explore the notion above, we present **CrissCross**, a self-supervised framework to learn robust generalized audio-visual representations from videos. CrissCross is built upon SimSiam (Chen and He 2021) to jointly learn self-supervised audio-visual representations through a mixture of intra- and cross-modal optimizations. In addition to learning intra-modal and standard synchronous cross-modal relations, CrissCross introduces the novel idea of learning cross-modal representations through *relaxing* time-synchronicity between corresponding audio and visual segments. We refer to this as ‘asynchronous cross-modal’ optimization, a concept that has not been explored in prior works. We use 3 datasets of different sizes: Kinetics-Sound (Arandjelovic and Zisserman 2017), Kinetics400 (Kay et al. 2017), and AudioSet (Gemmeke et al. 2017), to pretrain CrissCross. We evaluate CrissCross on different downstream tasks, namely action recognition, sound classification, and action retrieval. We use 2 popular benchmarks UCF101 (Soomro, Zamir, and Shah 2012) and HMDB51 (Kuehne et al. 2011) to perform action recognition and retrieval, while ESC50 (Piczak 2015) and DCASE (Stowell et al. 2015) are used for sound classification.

The key contributions of this work are as follows:

- We present a novel framework for multi-modal self-supervised learning by relaxing the audio-visual temporal synchronicity to learn effective generalized representations. Our method is simple, data efficient and less resource intensive, yet learns robust multi-modal representations for a variety of downstream tasks.
- We perform an in-depth study to explore the performance

of the proposed framework and its major concepts. Moreover, we perform thorough analyses, both quantitatively and qualitatively, in different setups, showing the benefit of learning asynchronous cross-modal relations.

- Comparing the performance of our method to prior works, CrissCross achieves state-of-the-arts on UCF101, HMDB, ESC50, and DCASE when pretrained on Kinetics400. Moreover, when trained with AudioSet, CrissCross achieves better or competitive performances versus the current state-of-the-arts.
- Lastly, when pretrained on the small-scale Kinetics-Sound (Arandjelovic and Zisserman 2017), CrissCross outperforms fully-supervised pretraining (Ma et al. 2020) by 1.4% and 7.4%, as well as prior self-supervised state-of-the-art (Ma et al. 2020) by 11.1% and 19.9% on UCF101 and HMDB51 respectively. To the best of our knowledge, very few prior works have attempted to pre-train on such small datasets, and in fact, this is the first time where self-supervised pretraining outperforms full supervision on action recognition in this setup.

We hope our proposed self-supervised method can motivate researchers to further explore the notion of *asynchronous* multi-modal representation learning.

2 Related Work

2.1 Self-supervised Learning

Self-supervised learning aims to learn generalized representations of data without any human annotated labels through properly designed pseudo tasks (also known as pretext tasks). Self-supervised learning has recently drawn significant attention in different areas such as image (Chen et al. 2020; Chen and He 2021; Misra and Maaten 2020; Caron et al. 2020; Grill et al. 2020; Caron et al. 2018), video (Morgado, Vasconcelos, and Misra 2021; Morgado, Misra, and Vasconcelos 2021; Alwassel et al. 2020; Asano et al. 2020; Patrick et al. 2021a; Alayrac et al. 2020; Min et al. 2021), and wearable data (Sarkar and Etemad 2020b,a; Sarkar et al. 2020) analysis among others.

In self-supervised learning, the main focus of interest lies in designing novel pseudo-tasks to learn useful representations. We briefly mention some of the popular categories in the context of self-supervised video representation learning, namely, *i*) context-based, *ii*) generation-based, *iii*) clustering-based, and *iv*) contrastive learning-based. Various pretext tasks have been proposed in the literature exploring the spatio-temporal context of video frames, for example, temporal order prediction (Lee et al. 2017), puzzle solving (Kim, Cho, and Kweon 2019; Misra, Zitnick, and Hebert 2016; Ahsan, Madhok, and Essa 2019), rotation prediction (Jing et al. 2018), and others. Generation-based video feature learning methods refer to the process of learning feature representations through video generation (Vondrick, Pirsiavash, and Torralba 2016; Tulyakov et al. 2018; Saito, Matsumoto, and Saito 2017), video colorization (Tran et al. 2016), and frame or clip prediction (Mathieu, Couprie, and LeCun 2016; Reda et al. 2018; Babaeizadeh et al. 2018; Liang et al. 2017; Finn, Goodfellow, and Levine 2016), among a few others. Clustering-based approaches (Alwassel

et al. 2020; Asano et al. 2020) rely on self-labeling where data is fed to the network and the extracted feature embeddings are clustered using a classical clustering algorithm such as k-means, followed by using the cluster assignments as the pseudo-labels for training the neural network. The key concept of contrastive learning (Chen and He 2021; Misra and Maaten 2020; Grill et al. 2020; Caron et al. 2020; Morgado, Vasconcelos, and Misra 2021; Patrick et al. 2021a) is that in the embedding space, ‘positive’ samples should be similar to each other, and ‘negative’ samples should have discriminative properties. Using this concept, several prior works (Morgado, Vasconcelos, and Misra 2021; Morgado, Misra, and Vasconcelos 2021; Patrick et al. 2021a; Ma et al. 2020) have attempted to learn representations by minimizing the distance between positive pairs and maximizing the distance between negative pairs.

2.2 Audio-Visual Representation Learning

Typically in multi-modal self-supervised learning, multiple networks are jointly trained on the pseudo tasks towards maximizing the mutual information between multiple data streams (Alwassel et al. 2020; Morgado, Vasconcelos, and Misra 2021; Korbar, Tran, and Torresani 2018; Xu et al. 2019; Wang et al. 2021; Khare, Parthasarathy, and Sundaram 2021; Siriwardhana et al. 2020). Following, we briefly discuss some of the prior works (Korbar, Tran, and Torresani 2018; Alwassel et al. 2020; Morgado, Vasconcelos, and Misra 2021; Ma et al. 2020) on audio-visual representation learning. A multi-modal self-supervised task is introduced in AVTS (Korbar, Tran, and Torresani 2018), leveraging the natural synergy between audio-visual data. The network is trained to distinguish whether the given audio and visual sequences are ‘in sync’ or ‘out of sync’. In XDC (Alwassel et al. 2020), the authors introduce a framework to learn cross-modal representations through a self-labeling process. Specifically, cross-modal pseudo-labeling is performed where the pseudo-labels computed from audio embeddings are used to train the visual backbone, while the pseudo-labels computed using visual embeddings are used to train the audio network. A self-supervised learning framework based on contrastive learning is proposed in AVID (Morgado, Vasconcelos, and Misra 2021) to learn audio-visual representations from videos. AVID performs instance discrimination as the pretext task by maximizing the cross-modal agreement of the audio-visual segments in addition to visual similarity. Though earlier works focus on learning cross-modal relations while maintaining a tight synchronicity between the audio and visual data, our proposed framework also considers asynchronous cross-modal relationships in addition to the standard synchronous relations.

3 Method

3.1 Approach

Let be given v , a sequence of visual frames, and a , the corresponding audio waveform. We can obtain n augmented views of v as $\{v_i\}_{i=0}^n$, and equal number of augmented views of a as $\{a_i\}_{i=0}^n$. A common way to learn individual representations from v and a is to minimize the em-

bedding distances (\mathcal{D}) between the augmented views of the each modality as $\mathcal{L}_{vv} = \sum_{i,j=0,i \neq j}^n \mathcal{D}(v_i, v_j)$ and $\mathcal{L}_{aa} = \sum_{i,j=0,i \neq j}^n \mathcal{D}(a_i, a_j)$ respectively in a self-supervised setting (Caron et al. 2020; Bardes, Ponce, and LeCun 2021; Chen and He 2021; Grill et al. 2020; Niizumi et al. 2021). Further, to learn multi-modal representations from $\{v, a\}$, a standard technique is to simply optimize a joint intra-modal loss $\mathcal{L}_{intra} = \mathcal{L}_{vv} + \mathcal{L}_{aa}$. Prior works (Alwassel et al. 2020; Morgado, Vasconcelos, and Misra 2021; Morgado, Misra, and Vasconcelos 2021) have demonstrated that in addition to \mathcal{L}_{intra} , a cross-modal optimization can be performed directly across visual and audio segments to further learn strong joint representations as $\mathcal{L}_{av} = \sum_{i=0}^n \mathcal{D}(a_i, v_i)$.

All of these learning procedures maintain a tight synchronicity between the two modalities, given that both a_i and v_i are segmented from the same timestamps. We conjecture, however, that *relaxing the synchronicity between modalities by a reasonable margin will enable more generalized representations to be learned* across time, to achieve better and more robust performance. Accordingly, we introduce asynchronous cross-modal loss \mathcal{L}_{async} , which exploits the relationship between audio and visual segments sampled at different timestamps. We define the final objective as $\mathcal{L}_{CrissCross}$ which exploits the combination of \mathcal{L}_{intra} , synchronous \mathcal{L}_{av} (which we refer to as \mathcal{L}_{sync}), and \mathcal{L}_{async} in an attempt to learn more generalized representations. While we present the detailed experiments and analysis of our proposed approach in the subsequent sections of the paper, here we perform a quick visualization to demonstrate the benefits of this concept. Figure 1 depicts the distributions of representations learned with and without \mathcal{L}_{async} , demonstrating that indeed relaxing the tight synchronicity helps in widening the distribution of the learned representations which could result in improved performance in a wide variety of downstream tasks.

3.2 Training Objective

To accomplish the notion above, let's define two neural networks, a visual encoder f_v and an audio encoder f_a . Here, f_v and f_a are composed of convolutional backbones and MLP projection heads. Moreover, we adopt a Siamese (Bromley et al. 1993) representation learning setup, where the networks share weights on two or more inputs. Next, We obtain two augmented views of $v = \{v_t\}_{t=0}^T$, denoted by v_1 and v_2 , defined as $\{v_t\}_{t=t_1}^{t_1+t_v}$ and $\{v_t\}_{t=t_2}^{t_2+t_v}$ respectively. Here, v_1 and v_2 have a duration of t_v , and are sampled at times t_1 and t_2 respectively. Note that v_1 and v_2 are augmented differently. Similarly, two augmented views of $a = \{a_t\}_{t=0}^T$ can be obtained as a_1 and a_2 as $\{a_t\}_{t=t_1}^{t_1+t_a}$ and $\{a_t\}_{t=t_2}^{t_2+t_a}$, respectively. Next, to learn intra-modal representations, the distance between $f_v(v_1)$ and $f_v(v_2)$, as well as, $f_a(a_1)$ and $f_a(a_2)$ can be minimized to train f_v and f_a respectively. However, such a naive approach would lead to mode collapse as pointed out in (Grill et al. 2020; Niizumi et al. 2021; Chen and He 2021; Caron et al. 2020). To tackle this, we follow the technique proposed in (Chen and He 2021). In particular, we minimize the cosine embedding distance \mathcal{D} of two output vectors p and $S(z)$, where p is the output vector

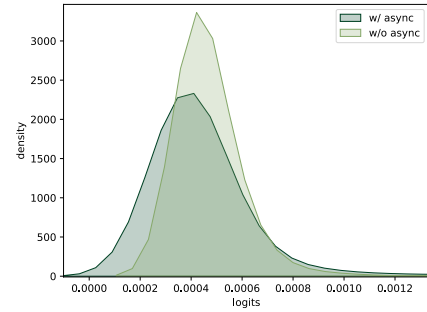


Figure 1: Distribution of the learned representations with and without the asynchronous cross-modal optimization.

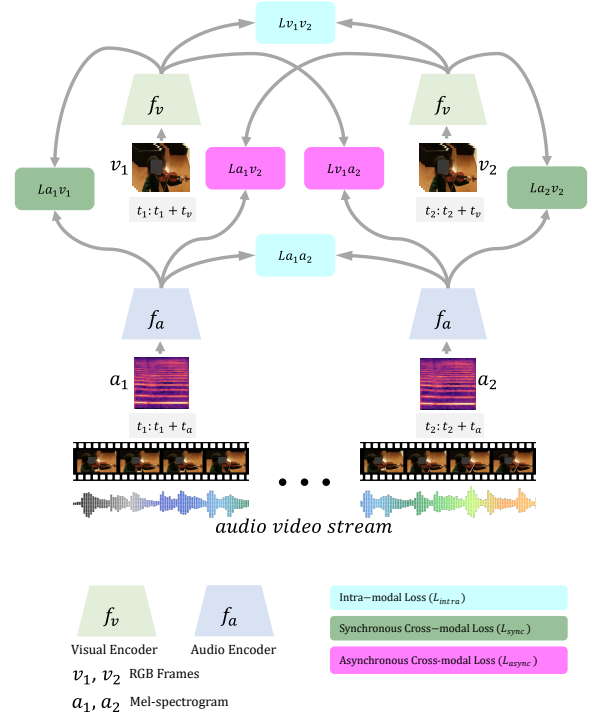


Figure 2: Our proposed framework. CrissCross learns strong audio-visual representations by exploiting intra-modal, as well as, sync. and async. cross-modal relations.

obtained from the predictor head and z represents the output vector obtained from the feature encoder followed by the stop-gradient operation. Here, the predictor head consists of an MLP head, which is used as an identity mapping, while the stop-gradient operation prevents the model from collapsing to a degenerated solution (Chen and He 2021). Here, \mathcal{D} is defined as:

$$\mathcal{D}(p, z) = -\frac{p}{\|p\|_2} \cdot \frac{z}{\|z\|_2}. \quad (1)$$

We use h_v and h_a as the predictor heads corresponding to visual and audio representations. Next, we obtain p_{v_1} and z_{v_2} as $h_v(f_v(v_1))$ and $S(f_v(v_2))$. Similarly, p_{a_1} and z_{a_2} are obtained as $h_a(f_a(a_1))$ and $S(f_a(a_2))$. To calculate the symmetrized loss, we further obtain p_{v_2} and z_{v_1} , as well as, p_{a_2}

and z_{a_1} . Therefore, to learn the intra-modal relations, we optimize the intra-modal loss \mathcal{L}_{intra} defined as:

$$\begin{aligned} \mathcal{L}_{intra} = & \left(\frac{1}{2} \mathcal{D}(p_{v_1}, S(z_{v_2})) + \frac{1}{2} \mathcal{D}(p_{v_2}, S(z_{v_1})) \right. \\ & \left. + \frac{1}{2} \mathcal{D}(p_{a_1}, S(z_{a_2})) + \frac{1}{2} \mathcal{D}(p_{a_2}, S(z_{a_1})) \right) / 2. \end{aligned} \quad (2)$$

Next, to learn synchronous cross-modal relations, we optimize the synchronous cross-modal loss \mathcal{L}_{sync} , defined as:

$$\begin{aligned} \mathcal{L}_{sync} = & \left(\frac{1}{2} \mathcal{D}(p_{v_1}, S(z_{a_1})) + \frac{1}{2} \mathcal{D}(p_{a_1}, S(z_{v_1})) \right. \\ & \left. + \frac{1}{2} \mathcal{D}(p_{v_2}, S(z_{a_2})) + \frac{1}{2} \mathcal{D}(p_{a_2}, S(z_{v_2})) \right) / 2. \end{aligned} \quad (3)$$

Additionally, based on our earlier intuition, to relax the temporal synchronicity, we minimize the distance between the audio and visual segments originated from different timestamps. We define asynchronous cross-modal loss \mathcal{L}_{async} as:

$$\begin{aligned} \mathcal{L}_{async} = & \left(\frac{1}{2} \mathcal{D}(p_{v_1}, S(z_{a_2})) + \frac{1}{2} \mathcal{D}(p_{a_2}, S(z_{v_1})) \right. \\ & \left. + \frac{1}{2} \mathcal{D}(p_{v_2}, S(z_{a_1})) + \frac{1}{2} \mathcal{D}(p_{a_1}, S(z_{v_2})) \right) / 2. \end{aligned} \quad (4)$$

Finally, to exploit intra-modal, as well as, synchronous and asynchronous cross-modal relations we define the final objective function as:

$$\mathcal{L}_{CrissCross} = \frac{1}{3} (\mathcal{L}_{intra} + \mathcal{L}_{sync} + \mathcal{L}_{async}). \quad (5)$$

We present the proposed CrissCross framework in Figure 2. Please note, for the sake of simplicity, we omit showing the stop-grad and predictor head connections in Figure 2. We present the pseudocode in Appendix A.

4 Experiments and Results

The details of the experiment setup and the findings of our thorough ablation studies investigating the major concepts of our proposed framework are presented here. Additionally, we extensively investigate a wide range of audio-visual augmentation techniques capable of learning strong audio-visual representations within our framework, the details are as follows.

4.1 Experiment Setup

Following the standard practice among the prior works (Morgado, Vasconcelos, and Misra 2021; Alwassel et al. 2020; Asano et al. 2020; Patrick et al. 2021a; Ma et al. 2020), we use Kinetics-Sound, Kinetics400, and AudioSet for pre-training. Additionally, Kinetics400, UCF101, HMDB51, ESC50 and DCASE are used for downstream evaluation. We use R(2+1)D (Tran et al. 2018) and ResNet (He et al. 2016) as the visual and audio backbones. To pretrain the network in a self-supervised fashion with audio-visual inputs, we downsample the visual streams to 16 frames per second and feed 8 frames of resolution 112^2 to the visual encoder. Next, we downsample the audio signals to 16kHz, and segment them into 2-second segments. We transform the segmented raw audio waveforms to mel-spectrograms using 80

Method	UCF101	ESC50
$\mathcal{L}_{v_1 v_2}$	69.1	-
$\mathcal{L}_{a_1 a_2}$	-	62.0
\mathcal{L}_{intra}	69.7	71.8
\mathcal{L}_{sync}	70.1	75.8
\mathcal{L}_{async}	69.1	74.8
$\mathcal{L}_{sync} + \mathcal{L}_{intra}$	73.8	78.0
$\mathcal{L}_{sync} + \mathcal{L}_{async}$	69.1	74.8
$\mathcal{L}_{async} + \mathcal{L}_{intra}$	72.4	75.3
$\mathcal{L}_{v_1 v_2} + \mathcal{L}_{sync} + \mathcal{L}_{async}$	71.3	78.5
$\mathcal{L}_{a_1 a_2} + \mathcal{L}_{sync} + \mathcal{L}_{async}$	70.8	75.3
$\mathcal{L}_{CrissCross}$	74.8	79.0

Table 1: We present the top-1 accuracy of CrissCross and its ablation variants, pretrained on Kinetics-Sound.

Pretrain	Downstream	w/o \mathcal{L}_{async}	w/ \mathcal{L}_{async}
KS	UCF101	73.8(↓ 1.0)	74.8
KS	ESC50	78.0(↓ 1.0)	79.0
K400	UCF101	75.8(↓ 4.1)	79.9
K400	ESC50	78.5(↓ 3.5)	82.0
K400	KS (a)	43.2(↓ 3.9)	47.1
K400	KS (v)	53.3(↓ 2.4)	55.7
K400	KS (a+v)	65.0(↓ 1.7)	66.7

Table 2: Impact of \mathcal{L}_{async} optimization in different pretraining and evaluation setups. Here, K400: Kinetics400, KS: Kinetics-Sound.

mel filters, we set the hop size as 10 milliseconds and FFT window length as 1024. Finally, we feed spectrograms of shape 80×200 to the audio encoder. We use Adam (Kingma and Ba 2015) optimizer with a cosine learning rate scheduler (Loshchilov and Hutter 2017) to pretrain the encoders and use a fixed learning rate to train the predictors. Please note that during the design exploration, we use Kinetics-Sound for pretraining, while the downstream evaluations are performed on UCF101 and ESC50 unless stated otherwise. We perform linear evaluations using 8 frames of visual input and 2 seconds of audio input. Next, a linear SVM classifier is trained using the extracted features, and report the top-1 accuracy for sample-level predictions. We provide the additional details of the experiment setup, datasets, architectures, and evaluation protocols in the Appendix.

4.2 Ablation Study

We present the ablation results in Tables 1 and 2 to show the improvements made by optimizing asynchronous cross-modal loss in addition to intra-modal and synchronous cross-modal losses. First, using Kinetics-Sound, we train the framework in uni-modal setups, denoted as $\mathcal{L}_{v_1 v_2}$ and $\mathcal{L}_{a_1 a_2}$. We report the top-1 accuracy of UCF101 and ESC50 as 69.1% and 62.0% respectively. Next, we train the network in a multi-modal setup, where we find that \mathcal{L}_{sync} outperforms the other multi-modal variants including \mathcal{L}_{intra} and \mathcal{L}_{async} , as well as, uni-modal baselines $\mathcal{L}_{v_1 v_2}$ and $\mathcal{L}_{a_1 a_2}$.

Further study shows that combining all the multi-modal losses improves the model performance. $\mathcal{L}_{CrissCross}$ outperforms \mathcal{L}_{sync} by 4.7% and 3.2% on action recognition and sound classification, respectively.

Further, to study the effect of \mathcal{L}_{async} in particular, we perform ablation studies using small-scale Kinetics-Sound and large-scale Kinetics400. We present the results in Table 2, where we observe that \mathcal{L}_{async} improves the performance on both the pretraining datasets. In particular, while pretrained on Kinetics400, optimizing \mathcal{L}_{async} in addition to \mathcal{L}_{sync} and \mathcal{L}_{intra} improves the performances by 4.1% and 3.5% on action recognition and sound classification respectively, showing the significance of asynchronous cross-modal optimization in a multi-modal setup. While pretrained on Kinetics-Sound, adding \mathcal{L}_{async} improves the performances by 1% on both the UCF101 and ESC50. We interestingly find that learning asynchronous cross-modal loss significantly improves the model performance when pretrained on large-scale Kinetics400. Our intuition is that as Kinetics-Sound consists of a few hand-picked classes which are prominently manifested in both audio and visual modalities, the performance gain due to \mathcal{L}_{async} is less prominent. However, Kinetics400 is considerably larger in scale and comprises highly diverse action classes which are not always very prominent both audibly and visually. It therefore benefits more from the generalized representations learned by asynchronous cross-modal optimization. Moreover, to demonstrate the benefit of optimizing \mathcal{L}_{async} throughout the pre-training process, we present the top-1 accuracy vs. pretraining epoch in Figure 4. It shows that \mathcal{L}_{async} significantly improves the model performance throughout the pretraining.

Multi-modal fusion. Next, we investigate if learning asynchronous cross-modal relations helps in multi-modal fusion. To test this, we use Kinetics-Sound as the downstream dataset and Kinetics400 as the pretraining dataset. We choose Kinetics-Sound for downstream evaluation as it consists of action classes that are represented prominently in both audio and visual domains. The results are presented in Table 2, where it is shown that learning asynchronous cross-modal relations improves multi-modal fusion by 1.7%. Additionally, we show the linear evaluation results obtained from the uni-modal feature representations for reference. It shows that optimizing \mathcal{L}_{async} improves the action classification accuracy by 2.4% and 3.9% using visual and audio representations, respectively.

Qualitative analysis. Lastly, to perform a qualitative analysis on the impact of \mathcal{L}_{async} we visualize the saliency maps obtained from the models when pretrained with and without the presence of the asynchronous loss. In this experiment, we directly use the models pretrained on Kinetics400 and use Grad-CAM (Omeiza et al. 2019) to visualize randomly selected samples from Kinetics400. A few examples are presented in Figure 3, where we observe that learning asynchronous relations helps the model focus better on the salient information. Specifically, we notice that optimizing \mathcal{L}_{async} helps in correctly locating the sound sources on the visual streams, as shown by the examples of ‘dribbling basketball’, ‘laughing’, ‘tapping guitar’, etc.

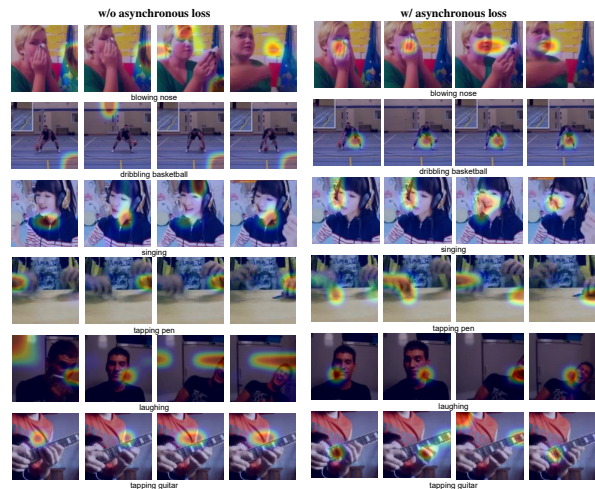


Figure 3: Visualization of saliency maps while pretrained without (left) and with (right) asynchronous loss.

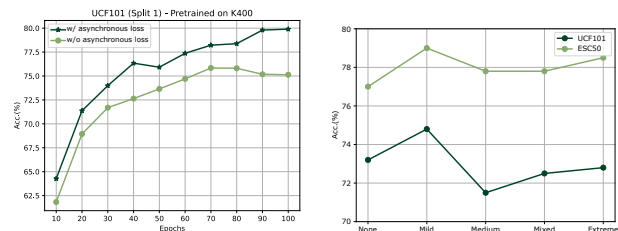


Figure 4: Left: Linear eval. top-1 acc. vs. pretraining epochs. Right: Exploring different temporal relaxation techniques.

4.3 Exploring Relaxed Time-synchronicity

Audio and visual modalities from the same source clip generally maintain a very strong correlation, which makes them suitable for multi-modal representation learning as one modality can be used as a supervisory signal for the other in a self-supervised setup. However, our intuition behind Criss-Cross is that these cross-modal temporal correlations do not necessarily need to follow a strict frame-wise coupling. Instead, we hypothesize that relaxing cross-modal temporal synchronicity to some extent can help in learning more generalized representations.

To facilitate this idea within CrissCross, we exploit 5 different temporal sampling methods to explore varying amounts of temporal synchronicity when learning cross-modal relationships. (i) *None*: where both the audio and visual segments are sampled from the exact same time window. (ii) *Mild*: where the two views of the audio-visual segments share 50% overlap amongst them. (iii) *Medium*: where adjacent frame sequences and audio segments are sampled. (iv) *Extreme*: in which we sample one view from the first half of the source clip, while the other view is sampled from the second half of the source clip. (v) *Mixed*: where the two audio-visual segments are sampled in a temporally random manner. The results presented in Figure 4 show that the *mild* relaxation works best for both action

	$lr_p = lr_b$	comm. pred.	2 layers proj.	default
UCF101	59.0	73.6	72.4	74.8
ESC50	62.3	75.3	75.0	79.0

Table 3: A comparative study of different predictor and projector setups. Here, lr_b : base LR and lr_p : pred LR

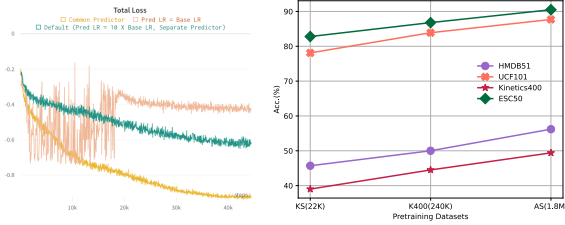


Figure 5: Left: Pretraining loss curves during predictor head design exploration. Right: Linear evaluation top-1 accuracy vs. pretraining dataset (size).

recognition and sound classification. Interestingly, we find that *medium* relaxation shows worse performance in comparison to others, whereas, *extreme* relaxation works somewhat well in our setup.

4.4 Exploring Design Choices

Predictor. Our empirical study shows that the predictor head plays an important role in effectively training the audio and visual encoders to learn good representations. The predictor architecture is similar to (Chen and He 2021). For the sake of completeness, we provide the details of the predictor head in Appendix F. We explore (i) different learning rates, and (ii) using a common vs. a separate predictor in the multi-modal setup. It should be noted that none of the variants cause a collapse, even though we notice considerable differences in performance. We present the findings below.

Following (Chen and He 2021), we use a constant learning rate for the predictors. However, unlike (Chen and He 2021), where the predictor learning rate is the same as the base learning rate of the encoder, we find that a higher predictor learning rate helps the network to learn better representations. In particular, setting the predictor learning rate to be the same as the base learning rate results in unstable training, and the loss curve shows oscillating behavior. We empirically find that setting the predictor learning rate to 10 times the base learning rate works well. We present the results in Table 3 and training curves in Figure 5.

Next, we evaluate whether the framework can be trained with a common predictor head instead of separate predictor heads (default setup). In simple terms, one predictor head would work towards identity mapping for both audio and visual feature vectors. To test this, l2-normalized feature vectors $f_v(v)$ and $f_a(a)$ are fed to the predictor, which are then used in a usual manner to optimize the cost function. The results are presented in Table 3. We observe that though such a setup works somewhat well, having separate predictors is beneficial for learning better representations. We present the

	Pretraining Dataset		
	KS (22K)	K400 (240K)	AS (1.8M)
HMDB51	45.7	50.0	56.2
UCF101	78.1	83.9	87.7
Kinetics400	39.0	44.5	50.1
ESC50	82.8	86.8	90.5
DCASE	93.0	96.0	97.0

Table 4: We present the top-1 acc. of linear evaluation on action recognition and sound classification.

training curves in Figure 5, it shows using common predictor head results in training losses saturate very quickly ultimately yielding worse performance compared to the use of separate predictor heads.

Projector. We present a comparative study of projection heads with 2 layers vs. 3 layers (default setup). We notice 2.4% and 4% improvements in top-1 accuracies when using 3 layers instead of 2 on action recognition and sound classification respectively (please see Table 3). The architecture details are presented in Appendix F.

4.5 Exploring Audio-Visual Augmentations.

We perform an in-depth study to explore the impact of different audio and visual augmentations.

Visual Augmentations. We explore a wide range of visual augmentations. As a starting point, we adopt the basic spatial augmentations used in (Morgado, Vasconcelos, and Misra 2021), which consists of Multi-Scale Crop (MSC), Horizontal Flip (HF), and Color Jitter (CJ). Additionally, we explore other augmentations, namely Gray Scale (GS), Gaussian Blur (GB) (Chen et al. 2020), and Cutout (C) (DeVries and Taylor 2017), which show great performance in image-based self-supervised learning (Chen et al. 2020; Van Gansbeke et al. 2020). We explore almost all the possible combinations of different visual augmentations in a uni-modal setup and present the results in Table 5. The results show that strong augmentations improve the top-1 accuracy by 6.8% in comparison to basic augmentations used in (Morgado, Vasconcelos, and Misra 2021).

Temporal Consistency of Spatial Augmentations. While investigating different spatial augmentations, we are also interested to know if the spatial augmentations should be consistent at the frame level or whether they should be random (i.e., vary among consecutive frames within a sequence). We refer to these concepts as *temporarily consistent* or *temporarily random*. We perform an experiment where we apply MSC-HF-CJ-GS randomly at the frame level and compare the results to applying the same augmentations consistently across all the frames of a sequence. Our results show that maintaining temporal consistency in spatial augmentations across consecutive frames is beneficial, which is in line with the findings in (Qian et al. 2021). Specifically, *Temporarily random* augmentations, results in top-1 accuracy of 53.69%, whereas, the same augmentations applied in a *temporarily consistent* manner results in 68.09%.

	Visual	UCF101	Audio	ESC50
Uni	MSC-HF-CJ	62.3	VJ	44.8
	MSC-HF-CJ-GS	68.1	VJ-M	49.5
	MSC-HF-CJ-GS-C	68.3	VJ-M-TW	49.5
	MSC-HF-CJ-GS-GB	68.7	VJ-M-RC	62.0
	MSC-HF-CJ-GS-GB-C	69.1		
	Visual + Audio	UCF101	ESC50	
Multi	MSC-HF-CJ-GS-C + VJ-M-RC	73.9	79.0	
	MSC-HF-CJ-GS-GB + VJ-M-RC	73.5	79.0	
	MSC-HF-CJ-GS-GB-C + VJ-M-RC	74.8	79.0	

Table 5: Exploring audio-visual augmentations.

Audio Augmentations. Similar to visual augmentations, we thoroughly investigate a variety of audio augmentations. Our audio augmentations include, Volume Jitter (VJ), Time and Frequency Masking (Mask) (Park et al. 2019), Random Crop (RC) (Niizumi et al. 2021), and Time Warping (TW) (Park et al. 2019). We also explore almost all the possible combinations of these augmentations and present the results in Table 5. Our findings show that time-frequency masking and random crop improve the top-1 accuracy by 17.25% compared to the base variant. We also notice that time warping doesn’t improve performance and is also quite computationally expensive. Hence, going forward we do not use time warping during pretraining.

Audio-Visual Augmentations. We conduct further experiments on a few combinations of augmentations in a *multi-modal* setup. We pick the top-performing augmentations obtained from the uni-modal variants and apply them concurrently. The results are presented in Table 5 where we find that the results are consistent with the uni-modal setups, as the combination of MSC-HF-CJ-GS-GB-C and VJ-M-RC performs the best in comparison to the other combinations. Finally, We summarize the augmentation schemes used for pretraining and evaluation in Tables S4 and S3.

4.6 Linear Evaluation and Scalability

To evaluate the quality of the representations learned through pretraining, we perform linear evaluation on action recognition (HMDB51, UCF101, and Kinetics400) and sound classification (ESC50 and DCASE). As mentioned, we use 3 different-sized datasets, i.e., Kinetics-Sound, Kinetics400, and AudioSet for pretraining. In Table 4 we report the top-1 accuracies averaged over all the splits. Moreover, to evaluate the scalability of CrissCross, we plot the linear evaluation results against the size of pretraining data as shown in Figure 5. We notice a steady improvement in performance as the dataset size increases, which shows CrissCross can likely be scaled on even larger datasets like IG65M (Ghadiyaram, Tran, and Mahajan 2019). Please note that in order to evaluate scalability we choose linear evaluation accuracy instead of full-finetuning as it gives more accurate measurements of learned representations obtained through self-supervised pretraining. In Figure 5, we do not include DCASE as it is a very small dataset (total of 100 recordings spread over 10 classes) and already reached very high accuracy on both Kinetics400 and AudioSet.

Method	Compute	Backbone (#Params (M))	U101	H51
Pretrained Dataset: Kinetics-Sound (Finetune input 32×224^2)				
CM-ACC(2020)	40 GPUs	3D-ResNet18 (33.4)	77.2	40.6
CrissCross	4 GPUs	R(2+1)D-18 (15.4)	88.3	60.5
Supervised (2020)	-	3D-ResNet18 (33.4)	86.9	53.1
Pretrained Dataset: Kinetics400 (Finetune input 8×224^2)				
XDC (2020)	64 GPUs	R(2+1)D-18 (31.5)	74.2	39.0
AVID (2021)	64 GPUs	R(2+1)D-18 (15.4)	83.7	49.5
Robust-xID (2021)	8 GPUs	R(2+1)D-18 (15.4)	81.9	49.5
CrissCross	8 GPUs	R(2+1)D-18 (15.4)	86.9	54.3
Pretrained Dataset: Kinetics400 (Finetune input 32×224^2)				
SeLaVi (2020)	64 GPUs	R(2+1)D-18 (31.5)	83.1	47.1
XDC (2020)	64 GPUs	R(2+1)D-18 (31.5)	86.8	52.6
CM-ACC* (2020)	40 GPUs	3D-ResNet18 (33.4)	90.2	61.8
AVID (2021)	64 GPUs	R(2+1)D-18 (15.4)	87.5	60.8
GDT (2021a)	64 GPUs	R(2+1)D-18 (31.5)	90.9	62.3
CMAC (2021)	8 GPUs	R(2+1)D-18 (31.5)	90.3	61.1
Robust-xID (2021)	8 GPUs	R(2+1)D-18 (15.4)	85.6	55.0
CrissCross	8 GPUs	R(2+1)D-18 (15.4)	91.5	64.7
Supervised (2021a)	-	R(2+1)D-18 (31.5)	95.0	74.0
Pretrained Dataset: AudioSet (Finetune input 8×224^2)				
XDC (2020)	64 GPUs	R(2+1)D-18 (31.5)	84.9	48.8
AVID (2021)	64 GPUs	R(2+1)D-18 (15.4)	88.6	57.6
CrissCross	8 GPUs	R(2+1)D-18 (15.4)	89.4	58.3
Pretrained Dataset: AudioSet (Finetune input 32×224^2)				
XDC (2020)	64 GPUs	R(2+1)D-18 (31.5)	93.0	63.7
MMV (2020)	32 TPUs	R(2+1)D-18 (31.5)	91.5	70.1
CM-ACC (2020)	40 GPUs	R(2+1)D-18 (33.4)	93.5	67.2
BraVe** (2021)	16 TPUs	R(2+1)D-18 (31.5)	93.6	70.8
AVID (2021)	64 GPUs	R(2+1)D-18 (15.4)	91.5	64.7
CrissCross	8 GPUs	R(2+1)D-18 (15.4)	92.4	67.4
Supervised (2021)	-	R(2+1)D-18 (31.5)	96.8	75.9

* refers to 240K samples from Kinetics700. ** pretrained with very high temporal resolutions (2 views of 32 & 128 frames) compared to others (8/16/32).

Table 6: SOTA comparison on action recognition.

4.7 Comparison to the State-of-the-Arts

Action Recognition. In line with (Alwassel et al. 2020; Asano et al. 2020; Morgado, Vasconcelos, and Misra 2021; Patrick et al. 2021a; Ma et al. 2020), we benchmark CrissCross using UCF101 and HMDB51 on action recognition. For a fair comparison to earlier works, we adopt 2 setups for finetuning, once with 8 frames, and the other with 32 frames. In both these setups, we use a spatial resolution of 224^2 . We tune the model using the split-1 of both datasets and report the top-1 accuracy averaged over all the splits. We notice large variability in experimental setups in the literature in terms of different backbones (e.g., deeper ConvNets, Transformer-based architectures, etc.) (Piergiovanni, Angelova, and Ryoo 2020; Qian et al. 2021; Patrick et al. 2021b), pretraining inputs (e.g., the addition of optical flow or text in addition to audio-visual data, etc.) (Piergiovanni, Angelova, and Ryoo 2020; Qian et al. 2021; Alayrac et al. 2020), and pretraining datasets, making it impractical to compare to all the prior works. Following the inclusion criteria of earlier works (Patrick et al. 2021a; Alwassel et al. 2020; Morgado, Vasconcelos, and Misra 2021), we compare CrissCross with methods that use similar backbones, inputs, and pretraining datasets.

The comparison of CrissCross with recent works is presented in Table 6. When pretrained with Kinetics400, Criss-

Method	UCF101			HMDB51		
	R@1	R@5	R@20	R@1	R@5	R@20
ST Order (2018)	25.7	36.2	49.2	-	-	-
SpeedNet (2020)	13.0	28.1	49.5	-	-	-
Clip Order (2019)	14.1	30.3	51.1	7.6	22.9	48.8
VCP (2020)	18.6	33.6	53.5	7.6	24.4	53.6
VSP (2020)	24.6	41.9	76.9	10.3	26.6	54.6
CoCLR (2020)	55.9	70.8	82.5	26.1	45.8	69.7
SeLaVi (2020)	52.0	68.6	84.5	24.8	47.6	75.5
Robust-xID (2021)	60.9	79.4	90.8	30.8	55.8	79.7
GDT (2021a)	57.4	73.4	88.1	25.4	51.4	75.0
CrissCross	63.8	78.7	89.9	26.4	50.5	77.7

Table 7: SOTA comparison on action retrieval.

Method	ESC50		DCASE	
	K400	AS	K400	AS
AVTS (2018)	76.7	80.6	91	93
XDC (2020)	78.0	84.8	91	95
AVID (2021)	79.1	89.1	93	96
MMV (2020)	-	85.6	-	-
BraVe (2021)	-	90.4	-	-
CrissCross	86.8	90.5	96	97

Table 8: SOTA comparison on sound classification.

Cross outperforms all the prior works by considerable margins on UCF101 and HMDB51 in both the fine-tuning setups. Moreover, CrissCross outperforms the current state-of-the-art AVID (Morgado, Vasconcelos, and Misra 2021), when pretrained on AudioSet and fine-tuned with 8-frame inputs, on both the UCF101 and HMDB51. When fine-tuned with 32-frame inputs, CrissCross achieves competitive results amongst the leading methods. We note that some of the prior works show slightly better performance compared to ours in some settings. We conjecture this to be due to the use of higher spatio-temporal resolution pretraining inputs in these models. E.g., BraVe (Recasens et al. 2021) is pretrained with 2 views of 32×112^2 and 128×112^2 , and the input size for MMV (Alayrac et al. 2020) and CM-ACC (Ma et al. 2020) are 32×224^2 and 16×224^2 , respectively. In comparison, CrissCross is pretrained with visual inputs of size 8×112^2 . However, we expect the performance of our model to improve further by using such higher resolutions, given the trend shown in (Recasens et al. 2021).

In addition to the commonly used Kinetics400 and AudioSet, we further evaluate CrissCross while pretrained on the small-scale Kinetics-Sound. Here, we observe significant improvements compared to the current state-of-the-art CM-ACC (Ma et al. 2020) on both UCF101 (88.3 vs. 77.2) and HMDB51 (60.5 vs. 40.6). Additionally, CrissCross outperforms fully-supervised pretraining by 1.4% and 7.4% on UCF101 and HMDB51 respectively when both the fully-supervised and self-supervised methods are pretrained on Kinetics-Sound. To the best of our knowledge, this is the first time that self-supervision outperforms full-supervised

pretraining on action recognition using the same small-scale pretraining dataset, showing that our method performs well on limited pretraining data.

Action Retrieval. In addition to full finetuning, we also compare the performance of CrissCross in an unsupervised setup. Following prior works (Morgado, Misra, and Vasconcelos 2021; Patrick et al. 2021a; Asano et al. 2020), we perform action retrieval using the split-1 of both UCF101 and HMDB51. The results are presented in Table 7 shows that CrissCross outperforms the current state-of-the-arts on UCF101 while achieving competitive results for HMDB51.

Sound Classification. We use two popular benchmarks ESC50 and DCASE to perform sound classification. We find large variability of experimental setups in the literature for evaluating audio representations. For instance, different backbones, input lengths, datasets, and evaluation protocols (linear evaluation, full-finetuning) have been used, making it impractical to compare to all the prior works. Following (Recasens et al. 2021; Alayrac et al. 2020), we perform linear evaluations using 5-second inputs on ESC50 and 1-second input for DCASE. As presented in Table 8, CrissCross outperforms current state-of-the-art AVID (Morgado, Vasconcelos, and Misra 2021) and BraVe (Recasens et al. 2021) on ESC50, while pretrained on Kinetics400 and AudioSet respectively. Additionally, CrissCross sets new state-of-the-art by outperforming all the prior works on DCASE when pretrained on both Kinetics400 and AudioSet.

5 Summary

We propose a novel self-supervised framework to learn audio-visual representations by exploiting intra-modal, as well as, synchronous and *asynchronous* cross-modal relationships. We conduct a thorough study investigating the major concepts of our framework. Our findings show that relaxation of cross-modal temporal synchronicity is beneficial for learning effective audio-visual representations. These representations can then be used for a variety of downstream tasks including action recognition, sound classification, and action retrieval.

Acknowledgments We are grateful to the Bank of Montreal and Mitacs for funding this research. We are thankful to SciNet HPC Consortium for helping with the computation resources.

References

- Ahsan, U.; Madhok, R.; and Essa, I. 2019. Video jigsaw: Unsupervised learning of spatiotemporal context for video action recognition. In *WACV*, 179–189.
- Alayrac, J.-B.; Recasens, A.; Schneider, R.; Arandjelovic, R.; Ramapuram, J.; De Fauw, J.; Smaira, L.; Dieleman, S.; and Zisserman, A. 2020. Self-Supervised MultiModal Versatile Networks. *NeurIPS*, 2(6): 7.
- Alwassel, H.; Mahajan, D.; Korbar, B.; Torresani, L.; Ghanem, B.; and Tran, D. 2020. Self-Supervised Learning by Cross-Modal Audio-Video Clustering. *NerulPS*, 33.

- Arandjelovic, R.; and Zisserman, A. 2017. Look, listen and learn. In *ICCV*, 609–617.
- Asano, Y. M.; Patrick, M.; Rupprecht, C.; and Vedaldi, A. 2020. Labelling unlabelled videos from scratch with multi-modal self-supervision. In *NeurIPS*.
- Babaeizadeh, M.; Finn, C.; Erhan, D.; Campbell, R. H.; and Levine, S. 2018. Stochastic Variational Video Prediction. In *ICLR*.
- Bardes, A.; Ponce, J.; and LeCun, Y. 2021. Vireg: Variance-invariance-covariance regularization for self-supervised learning. *arXiv preprint arXiv:2105.04906*.
- Benaïm, S.; Ephrat, A.; Lang, O.; Mosseri, I.; Freeman, W. T.; Rubinstein, M.; Irani, M.; and Dekel, T. 2020. Speednet: Learning the speediness in videos. In *CVPR*, 9922–9931.
- Bromley, J.; Guyon, I.; LeCun, Y.; Säckinger, E.; and Shah, R. 1993. Signature verification using a "siamese" time delay neural network. *Advances in neural information processing systems*, 6.
- Buchler, U.; Brattoli, B.; and Ommer, B. 2018. Improving spatiotemporal self-supervision by deep reinforcement learning. In *ECCV*.
- Caron, M.; Bojanowski, P.; Joulin, A.; and Douze, M. 2018. Deep clustering for unsupervised learning of visual features. In *ECCV*, 132–149.
- Caron, M.; Misra, I.; Mairal, J.; Goyal, P.; Bojanowski, P.; and Joulin, A. 2020. Unsupervised Learning of Visual Features by Contrasting Cluster Assignments. In *NeurIPS*.
- Chen, T.; Kornblith, S.; Norouzi, M.; and Hinton, G. 2020. A simple framework for contrastive learning of visual representations. In *ICML*, 1597–1607.
- Chen, X.; and He, K. 2021. Exploring simple siamese representation learning. In *CVPR*, 15750–15758.
- Cho, H.; Kim, T.; Chang, H. J.; and Hwang, W. 2020. Self-Supervised Spatio-Temporal Representation Learning Using Variable Playback Speed Prediction. *arXiv preprint arXiv:2003.02692*.
- DeVries, T.; and Taylor, G. W. 2017. Improved regularization of convolutional neural networks with cutout. *arXiv preprint arXiv:1708.04552*.
- Finn, C.; Goodfellow, I.; and Levine, S. 2016. Unsupervised learning for physical interaction through video prediction. *NeurIPS*, 29: 64–72.
- Gemmeke, J. F.; Ellis, D. P.; Freedman, D.; Jansen, A.; Lawrence, W.; Moore, R. C.; Plakal, M.; and Ritter, M. 2017. Audio set: An ontology and human-labeled dataset for audio events. In *ICASSP*, 776–780.
- Ghadiyaram, D.; Tran, D.; and Mahajan, D. 2019. Large-Scale Weakly-Supervised Pre-Training for Video Action Recognition. In *CVPR*, 12038–12047.
- Grill, J.-B.; Strub, F.; Altché, F.; Tallec, C.; Richemond, P.; Buchatskaya, E.; Doersch, C.; Pires, B.; Guo, Z.; Azar, M.; et al. 2020. Bootstrap Your Own Latent: A new approach to self-supervised learning. In *NeurIPS*.
- Han, T.; Xie, W.; and Zisserman, A. 2020. Self-supervised Co-training for Video Representation Learning. In *NeurIPS*.
- He, K.; Zhang, X.; Ren, S.; and Sun, J. 2016. Deep residual learning for image recognition. In *CVPR*, 770–778.
- Jing, L.; Yang, X.; Liu, J.; and Tian, Y. 2018. Self-supervised spatiotemporal feature learning via video rotation prediction. *arXiv preprint arXiv:1811.11387*.
- Kay, W.; Carreira, J.; Simonyan, K.; Zhang, B.; Hillier, C.; Vijayanarasimhan, S.; Viola, F.; Green, T.; Back, T.; Natsev, P.; et al. 2017. The kinetics human action video dataset. *arXiv preprint arXiv:1705.06950*.
- Khare, A.; Parthasarathy, S.; and Sundaram, S. 2021. Self-Supervised learning with cross-modal transformers for emotion recognition. In *SLT*, 381–388.
- Kim, D.; Cho, D.; and Kweon, I. S. 2019. Self-supervised video representation learning with space-time cubic puzzles. In *AAAI*, volume 33, 8545–8552.
- Kingma, D. P.; and Ba, J. 2015. Adam: A Method for Stochastic Optimization. In *ICLR*.
- Korbar, B.; Tran, D.; and Torresani, L. 2018. Cooperative learning of audio and video models from self-supervised synchronization. In *NeurIPS*, 7774–7785.
- Kuehne, H.; Jhuang, H.; Garrote, E.; Poggio, T.; and Serre, T. 2011. HMDB: a large video database for human motion recognition. In *ICCV*, 2556–2563.
- Lee, H.-Y.; Huang, J.-B.; Singh, M.; and Yang, M.-H. 2017. Unsupervised representation learning by sorting sequences. In *CVPR*.
- Liang, X.; Lee, L.; Dai, W.; and Xing, E. P. 2017. Dual motion gan for future-flow embedded video prediction. In *ICCV*, 1744–1752.
- Loshchilov, I.; and Hutter, F. 2017. Sgdr: Stochastic gradient descent with warm restarts. In *ICLR*.
- Luo, D.; Liu, C.; Zhou, Y.; Yang, D.; Ma, C.; Ye, Q.; and Wang, W. 2020. Video cloze procedure for self-supervised spatio-temporal learning. In *AAAI*.
- Ma, S.; Zeng, Z.; McDuff, D.; and Song, Y. 2020. Active Contrastive Learning of Audio-Visual Video Representations. In *ICLR*.
- Mathieu, M.; Couprie, C.; and LeCun, Y. 2016. Deep multi-scale video prediction beyond mean square error. In *ICLR*.
- McFee, B.; Raffel, C.; Liang, D.; Ellis, D. P.; McVicar, M.; Battenberg, E.; and Nieto, O. 2015. librosa: Audio and music signal analysis in python. In *Python in Science Conference*, volume 8, 18–25.
- Micikevicius, P.; Narang, S.; Alben, J.; Diamos, G.; Elsen, E.; Garcia, D.; Ginsburg, B.; Houston, M.; Kuchaiev, O.; Venkatesh, G.; et al. 2018. Mixed Precision Training. In *ICLR*.
- Min, S.; Dai, Q.; Xie, H.; Gan, C.; Zhang, Y.; and Wang, J. 2021. Cross-Modal Attention Consistency for Video-Audio Unsupervised Learning. *arXiv preprint arXiv:2106.06939*.
- Misra, I.; and Maaten, L. v. d. 2020. Self-supervised learning of pretext-invariant representations. In *CVPR*, 6707–6717.
- Misra, I.; Zitnick, C. L.; and Hebert, M. 2016. Shuffle and learn: unsupervised learning using temporal order verification. In *ECCV*, 527–544.

- Morgado, P.; Misra, I.; and Vasconcelos, N. 2021. Robust Audio-Visual Instance Discrimination. In *CVPR*, 12934–12945.
- Morgado, P.; Vasconcelos, N.; and Misra, I. 2021. Audio-visual instance discrimination with cross-modal agreement. In *CVPR*, 12475–12486.
- Niizumi, D.; Takeuchi, D.; Ohishi, Y.; Harada, N.; and Kashino, K. 2021. BYOL for Audio: Self-Supervised Learning for General-Purpose Audio Representation. *arXiv preprint arXiv:2103.06695*.
- Omeiza, D.; Speakman, S.; Cintas, C.; and Weldermariam, K. 2019. Smooth grad-cam++: An enhanced inference level visualization technique for deep convolutional neural network models. *arXiv preprint arXiv:1908.01224*.
- Park, D. S.; Chan, W.; Zhang, Y.; Chiu, C.-C.; Zoph, B.; Cubuk, E. D.; and Le, Q. V. 2019. SpecAugment: A simple data augmentation method for automatic speech recognition. *arXiv preprint arXiv:1904.08779*.
- Paszke, A.; Gross, S.; Massa, F.; Lerer, A.; Bradbury, J.; Chanan, G.; Killeen, T.; Lin, Z.; Gimelshein, N.; Antiga, L.; et al. 2019. Pytorch: An imperative style, high-performance deep learning library. *NeurIPS*, 32: 8026–8037.
- Patrick, M.; Asano, Y. M.; Kuznetsova, P.; Fong, R.; Henriques, J. F.; Zweig, G.; and Vedaldi, A. 2021a. On compositions of transformations in contrastive self-supervised learning. In *Proceedings of the IEEE/CVF International Conference on Computer Vision*, 9577–9587.
- Patrick, M.; Huang, P.-Y.; Misra, I.; Metze, F.; Vedaldi, A.; Asano, Y. M.; and Henriques, J. F. 2021b. Space-Time Crop & Attend: Improving Cross-modal Video Representation Learning. In *ICCV*, 10560–10572.
- Piczak, K. J. 2015. ESC: Dataset for Environmental Sound Classification. In *ACM Conference on Multimedia*, 1015–1018. .
- Piergiovanni, A.; Angelova, A.; and Ryoo, M. S. 2020. Evolving losses for unsupervised video representation learning. In *CVPR*, 133–142.
- Qian, R.; Meng, T.; Gong, B.; Yang, M.-H.; Wang, H.; Belongie, S.; and Cui, Y. 2021. Spatiotemporal contrastive video representation learning. In *CVPR*, 6964–6974.
- Recasens, A.; Luc, P.; Alayrac, J.-B.; Wang, L.; Strub, F.; Tallec, C.; Malinowski, M.; Patraucean, V.; Altché, F.; Valko, M.; et al. 2021. Broaden Your Views for Self-Supervised Video Learning. *arXiv preprint arXiv:2103.16559*.
- Reda, F. A.; Liu, G.; Shih, K. J.; Kirby, R.; Barker, J.; Tarjan, D.; Tao, A.; and Catanzaro, B. 2018. Sdc-net: Video prediction using spatially-displaced convolution. In *ECCV*, 718–733.
- Saito, M.; Matsumoto, E.; and Saito, S. 2017. Temporal generative adversarial nets with singular value clipping. In *ICCV*, 2830–2839.
- Sarkar, P.; and Etemad, A. 2020a. Self-supervised ECG representation learning for emotion recognition. *IEEE Transactions on Affective Computing*.
- Sarkar, P.; and Etemad, A. 2020b. Self-supervised learning for ecg-based emotion recognition. In *ICASSP*, 3217–3221.
- Sarkar, P.; Lobmaier, S.; Fabre, B.; Berg, G.; Mueller, A.; Frasch, M. G.; Antonelli, M. C.; and Etemad, A. 2020. Detection of Maternal and Fetal Stress from ECG with Self-supervised Representation Learning. *arXiv e-prints*, arXiv–2011.
- Siriwardhana, S.; Kaluarachchi, T.; Billingham, M.; and Nanayakkara, S. 2020. Multimodal Emotion Recognition With Transformer-Based Self Supervised Feature Fusion. *IEEE Access*, 8: 176274–176285.
- Soomro, K.; Zamir, A. R.; and Shah, M. 2012. UCF101: A dataset of 101 human actions classes from videos in the wild. *arXiv preprint arXiv:1212.0402*.
- Stowell, D.; Giannoulis, D.; Benetos, E.; Lagrange, M.; and Plumbley, M. D. 2015. Detection and classification of acoustic scenes and events. *IEEE Transactions on Multimedia*, 17(10): 1733–1746.
- Tran, D.; Bourdev, L.; Fergus, R.; Torresani, L.; and Paluri, M. 2016. Deep end2end voxel2voxel prediction. In *CVPRW*, 17–24.
- Tran, D.; Wang, H.; Torresani, L.; Ray, J.; LeCun, Y.; and Paluri, M. 2018. A closer look at spatiotemporal convolutions for action recognition. In *CVPR*, 6450–6459.
- Tulyakov, S.; Liu, M.-Y.; Yang, X.; and Kautz, J. 2018. MoCoGAN: Decomposing motion and content for video generation. In *CVPR*, 1526–1535.
- Van Gansbeke, W.; Vandenhende, S.; Georgoulis, S.; Proesmans, M.; and Van Gool, L. 2020. Scan: Learning to classify images without labels. In *ECCV*, 268–285.
- Vondrick, C.; Pirsaviash, H.; and Torralba, A. 2016. Generating videos with scene dynamics. *NeurIPS*, 29: 613–621.
- Wang, J.; Jiao, J.; Bao, L.; He, S.; Liu, W.; and Liu, Y.-H. 2021. Self-supervised Video Representation Learning by Uncovering Spatio-temporal Statistics. *PAMI*.
- Xu, D.; Xiao, J.; Zhao, Z.; Shao, J.; Xie, D.; and Zhuang, Y. 2019. Self-supervised spatiotemporal learning via video clip order prediction. In *CVPR*, 10334–10343.
- You, Y.; Gitman, I.; and Ginsburg, B. 2017. Large batch training of convolutional networks. *arXiv preprint arXiv:1708.03888*.

Supplementary Material

The organization of the supplementary material is as follows:

- Appendix A: Pseudocode;
- Appendix B: Qualitative Analysis;
- Appendix C: Datasets;
- Appendix D: Data Augmentations;
- Appendix E: Evaluation Protocols;
- Appendix G: Hyperparameters;
- Appendix F: Architectures;
- Appendix H: Limitations;
- Appendix I: Broader Impact.

A Pseudocode

We present the pseudocode of our proposed CrissCross framework in Algorithm 1.

Algorithm 1: CrissCross pseudocode (PyTorch style).

```

# fv: visual encoder (backbone+projection mlp)
# fa: audio encoder (backbone+projection mlp)
# hv: visual predictor head (prediction mlp)
# ha: audio predictor head (prediction mlp)
# D: loss function, following Eqn. 1

def forward(v1, v2, a1, a2):
    """
    v1, V2: minibatch of augmented visual samples
    a1, a2: minibatch of augmented audio samples
    """

    # visual
    zv1, zv2 = fv(v1), fv(v2) # visual embeddings
    pv1, pv2 = hv(zv1), hv(zv2) # predictor output

    # audio
    za1, za2 = fa(a1), fa(a2) # audio embeddings
    pa1, pa2 = ha(za1), ha(za2) # predictor output

    # loss calculation

    # intra-modal loss, following Eqn. 2
    L_intra = D(pv1, zv2)/2 + D(pv2, zv1)/2 + \
        D(pa1, za2)/2 + D(pa2, za1)/2

    # synchronous cross-modal loss, following Eqn. 3
    L_sync = (D(pv1, za1)/2 + D(pa1, zv1)/2 + Lv2a2 + \
        D(pv2, za2)/2 + D(pa2, zv2)/2)/2

    # asynchronous cross-modal loss, following Eqn. 4
    L_async = (D(pv1, za2)/2 + D(pa2, zv1)/2 + \
        D(pa1, zv2)/2 + D(pv2, za1)/2)/2

    # total loss, following Eqn. 5
    L_CrissCross = (L_async + L_sync + L_intra)/3

    return L_CrissCross

```

B Qualitative Analysis

To perform a qualitative analysis of the learned representations in an unsupervised setup, we present the nearest neighborhoods of video-to-video and audio-to-audio retrieval in Figures S1 and S2. In this experiment, we use Kinetics400 (Kay et al. 2017) to pretrain CrissCross. Next, we use the features extracted from randomly selected samples of the validation split to query the training features. We find that in most of the cases CrissCross performs fairly well, we notice very few instances of wrong retrieval, which generally



Figure S1: We present a few randomly selected samples of video-to-video retrieval. Here, the frames with black borders represent the query, and the next 5 frames represent the top-5 neighborhoods. The correct retrievals are marked with green, while the wrong ones are marked with red.

occur when the visual scenes or sound events are very similar. For instance, ‘playing piano’ and ‘playing organ’ for video-to-video retrieval and ‘playing keyboard’ and ‘playing xylophone’ for audio-to-audio retrieval.

C Datasets

C.1 Pretraining Datasets

We use 3 datasets of different sizes for pretraining, namely, Kinetics-Sound (Arandjelovic and Zisserman 2017), Kinetics400 (Kay et al. 2017), and AudioSet (Gemmeke et al. 2017). Kinetics-Sound is a small-scale action recognition dataset, which has a total of 22K video clips, distributed over 32 action classes. Kinetics400 is a medium-scale human action recognition dataset, originally collected from YouTube. It has a total of 240K training samples and 400

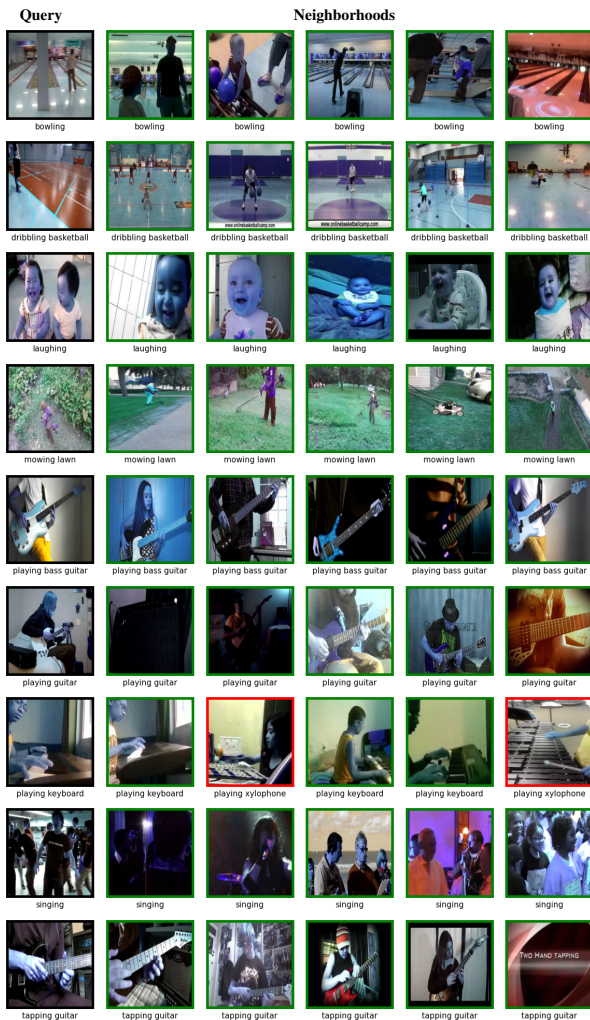


Figure S2: We present a few randomly selected samples of **audio-to-audio** retrieval. Here, the frames with black borders represent the query, and the next 5 frames represent the top-5 neighborhoods. The correct retrievals are marked with green, while the wrong ones are marked with red.

action classes. Please note that Kinetics-Sound is a subset of Kinetics400, and consists of action classes which are prominently manifested audibly and visually (Arandjelovic and Zisserman 2017). Lastly, AudioSet (Gemmeke et al. 2017) is a large-scale video dataset of audio events consisting of a total of 1.8M audio-video segments originally obtained from YouTube spread over 632 audio classes. Please note that none of the provided labels are used in self-supervised pretraining.

C.2 Downstream Datasets

Following the standard practices of prior works (Morgado, Vasconcelos, and Misra 2021; Morgado, Misra, and Vasconcelos 2021; Alayrac et al. 2020; Alwassel et al. 2020; Asano et al. 2020; Korbar, Tran, and Torresani 2018), we evaluate our self-supervised methods on two types of down-

stream tasks: (i) action recognition based on visual representations and (ii) sound classification based on audio representations. To perform action recognition, we use two popular benchmarks, i.e., UCF101 (Soomro, Zamir, and Shah 2012) and HMDB51 (Kuehne et al. 2011). UCF101 consists of a total of 13K clips distributed among 101 action classes, while HMDB contains nearly 7K video clips distributed over 51 action categories. To perform sound classification, we use two popular benchmarks ESC50 (Piczak 2015) and DCASE2014 (Stowell et al. 2015). ESC50 is a collection of 2K audio events comprised of 50 classes and DCASE2014 is an audio event dataset of 100 recordings spread over 10 categories.

D Data Augmentation

Here we present the details of the augmentation parameters for both visual and audio modalities.

D.1 Visual Augmentations

The parameters for visual augmentations are presented in Table S1. Some of the parameters are chosen from the literature, while the rest are found through empirical search. We set the parameters of Multi-Scale Crop, Gaussian Blur, and Gray Scale as suggested in (Chen et al. 2020), and the parameters for Color Jitter are taken from (Morgado, Vasconcelos, and Misra 2021). We use TorchVision (Paszke et al. 2019) for all the implementations of visual augmentations, except Cutout where we use the implementation available here¹. Please note that for the Cutout transformation, the mask is created with the mean value of the first frame in the sequence.

D.2 Audio Augmentations

We present the parameters used for audio augmentations in Table S2. We use the Librosa (McFee et al. 2015) library to generate mel-spectrograms. We use the techniques proposed in (Park et al. 2019) to perform Time Mask, Frequency Mask, and Time Warp transformations². The parameters for the audio augmentations are set empirically, except for Random Crop which we adopt from (Niizumi et al. 2021).

E Evaluation Protocol

To evaluate the representations learned with self-supervised pretraining, we test the proposed framework in different setups, namely linear evaluation, full finetuning, and retrieval. The details of the evaluation protocols are mentioned below.

E.1 Linear Evaluation

To perform linear evaluations of the learned representations on downstream tasks, we extract fixed features (also called frozen features) using the pretrained backbones. We train a linear classifier using the fixed feature representations. The details are presented below.

¹<https://github.com/uoguelph-mlrg/Cutout>

²<https://github.com/s3prl/s3prl>

Augmentation	Parameters
Multi Scale Crop	min area = 0.08
Horizontal Flip	p = 0.5
Color Jitter	brightness = 0.4 contrast = 0.4 saturation = 0.4 hue = 0.2
Gray Scale	p = 0.2
Gaussian Blur	p = 0.5
Cutout	max size = 20 num = 1

Table S1: Visual augmentation parameters.

Augmentation	Parameters
Volume Jitter	range = ± 0.2
Time Mask	max size = 20 num = 2
Frequency Mask	max size = 10 num = 2
Timewarp	wrap window = 20
Random Crop	range = [0.6, 1.5] crop scale = [1.0, 1.5]

Table S2: Audio augmentation parameters.

Action Recognition.

To perform linear evaluations on action recognition, we follow standard evaluation protocols laid out in prior works (Alayrac et al. 2020; Recasens et al. 2021; Patrick et al. 2021a; Morgado, Vasconcelos, and Misra 2021). The details are presented below.

HMDB51 and UCF101. We perform linear evaluations in 2 setups, i.e., 8-frame and 32-frame inputs. We evaluate on 8-frame inputs for the design explorations and 32-frame inputs for large-scale experiments.

Following the protocols mentioned in (Alayrac et al. 2020; Recasens et al. 2021), we feed 8-frame inputs to the video backbone, with a spatial resolution of 224^2 . During training, we randomly pick 25 clips per sample to extract augmented representations, while during testing, we uniformly select 10 clips per sample and report top-1 accuracy at sample-level prediction by averaging clip-level predictions. The augmentation techniques are mentioned in Section D. We don’t apply the Gaussian Blur while extracting the training features since it deteriorates the performance. Moreover, to perform a deterministic evaluation, we don’t apply any augmentations during validation. The visual features are extracted from the final convolution layer and passed to a max-pool layer with a kernel size of (1, 4, 4) (Morgado, Vasconcelos, and Misra 2021). Finally, we use the learned visual representations to train a linear SVM classifier, we sweep the cost values between {0.00001, 0.00005,

	MSC	HF	CJ	GS	GB	C
Pretraining	✓	✓	✓	✓	✓	✓
Full-finetune	✓	✓	✓	✓	✗	✓
Linear evaluation	✓	✓	✓	✓	✗	✓

Table S3: Audio augmentation summary.

	VJ	Mask	RC	TW
Pretraining	✓	✓	✓	✗
Linear evaluation	✓	✓	✓	✓

Table S4: Visual augmentation summary.

0.0001, 0.0005, 0.001, 0.005, 0.01, 1} and report the best accuracy.

When validating on 32-frame inputs, we could not perform SVM as the feature vector is too large to hold in the memory. Hence, we use a linear fully-connected layer at the end of the video backbone. Note that during training the backbone is kept frozen and only the linear layer is trained. we keep the rest of the setup the same as described earlier, with the exception of training where we randomly select 10 clips per sample.

Kinetics400. As Kinetics400 (Kay et al. 2017) is a large-scale dataset, the feature vector is too large to save in memory. Following (Morgado, Vasconcelos, and Misra 2021), we use a fully connected layer at the end of the frozen backbone and feed 8×224^2 frame inputs. During training, we randomly pick 1 clip per sample, while during validation, we uniformly select 10 clips per sample. Note that the rest of the setups remain the same, as described for HMDB51 and UCF101. Finally, we obtain the sample-level prediction by averaging the clip-level predictions and report the top-1 accuracy.

Sound Classification.

In case of evaluating audio representations, we follow the evaluation protocol laid out in prior works (Morgado, Vasconcelos, and Misra 2021; Alwassel et al. 2020; Alayrac et al. 2020; Recasens et al. 2021) for respective datasets. The details are mentioned below.

ESC50. We perform linear evaluations on ESC50 in 2 setups, we use 2-second audio input for design exploration and 5-second audio input for large-scale experiments. Following (Patrick et al. 2021a), we extract 10 epochs worth of augmented feature vectors from the training clips. During testing, when using 2-second inputs, we extract 10 equally spaced audio segments (Morgado, Vasconcelos, and Misra 2021; Patrick et al. 2021a; Alwassel et al. 2020), and when using 5-second inputs, we extract 1 segment (Alayrac et al. 2020; Recasens et al. 2021) from each sample. We perform the augmentations mentioned in Section D to extract the training features. We notice that unlike self-supervised pre-training, time warping improves the model performance in the linear evaluation. We do not apply any augmentations during validation. We extract the representations from the final convolution layer and pass it through a max-pool layer

with a kernel size of (1, 3) and a stride of (1, 2) (Patrick et al. 2021a). Similar to action recognition, we perform classification using a one-vs-all linear SVM classifier, we sweep the cost values between {0.00001, 0.00005, 0.0001, 0.0005, 0.001, 0.005, 0.01, 1} and report the best accuracy.

DCASE. To validate on DCASE, we follow the protocol mentioned in (Morgado, Vasconcelos, and Misra 2021). We extract 60 clips per sample and train a linear classifier on the extracted representations. Note that the augmentation and feature extraction schemes remain the same as mentioned for ESC50. We report the top-1 sample level accuracies by averaging the clip level predictions.

Multi-modal Fusion. To perform a multi-modal linear evaluation with late fusion, we extract features from Kinetics-Sound. During training, we randomly pick 10 audio-visual clips per sample, each 2 seconds long. Next, we extract feature vectors of dimension 2048 from the last convolution layer by using max-pooling with kernel sizes of (1, 2, 2) and (1, 4) for visual and audio respectively. Following, the feature vectors are concatenated to train a linear SVM classifier. Finally, we report the top-1 sample level accuracy for action classification.

E.2 Full Finetuning

Following earlier works (Alwassel et al. 2020; Morgado, Vasconcelos, and Misra 2021; Morgado, Misra, and Vasconcelos 2021; Asano et al. 2020), we use the pretrained visual backbone along with a newly added fully-connected layer for full finetuning on UCF101 (Soomro, Zamir, and Shah 2012) and HMDB51 (Kuehne et al. 2011). We adopt two setups for full finetuning, 8-frame inputs and 32-frame inputs. In both cases, we use a spatial resolution of 224^2 . Lastly, we replace the final adaptive average-pooling layer with an adaptive max-pooling layer. We find that applying strong augmentations improves the model performance in full-finetuning. Please see the augmentation details in Section D. During testing, we extract 10 equally spaced clips from each sample and do not apply any augmentations. We report the top-1 accuracy at sample-level prediction by averaging the clip-level predictions. We use an SGD optimizer with a multi-step learning rate scheduler to finetune the model. We present the hyperparameters of full-finetuning in Table S11.

E.3 Retrieval

We follow the protocol laid out in (Patrick et al. 2021a; Xu et al. 2019). We uniformly select 10 clips per sample from both training and test splits. We fit 2-second inputs to the backbone to extract representations. We empirically test additional steps such as l2-normalization and applying batch-normalization on the extracted features, and notice that they do not help the performance. Hence, we simply average the features extracted from the test split to query the features of the training split. We compute the cosine distance between the feature vectors of the test clips (query) and the representations of all the training clips (neighbors). We consider a correct prediction if k neighboring clips of a query clip belong to the same class. We calculate accuracies for

Layer	X_s	X_t	C	K_s	K_t	S_s	S_t
frames	112	8	3	-	-	-	-
conv1	56	8	64	7	3	2	1
maxpool	28	8	64	3	1	2	1
block2.1.1	28	8	64	3	3	1	1
block2.1.2	28	8	64	3	3	1	1
block2.2.1	28	8	64	3	3	1	1
block2.2.2	28	8	64	3	3	1	1
block3.1.1	14	4	128	3	3	2	2
block3.1.2	14	4	128	3	3	1	1
block3.2.1	14	4	128	3	3	1	1
block3.2.2	14	4	128	3	3	1	1
block4.1.1	7	2	256	3	3	2	2
block4.1.2	7	2	256	3	3	1	1
block4.2.1	7	2	256	3	3	1	1
block4.2.2	7	2	256	3	3	1	1
block5.1.1	4	1	512	3	3	2	2
block5.1.2	4	1	512	3	3	1	1
block5.2.1	4	1	512	3	3	1	1
block5.2.2	4	1	512	3	3	1	1
avg-pool	-	-	512	-	-	-	-

Table S5: Architecture of the video backbone: R(2+1)D-18.

$k = 1, 5, 20$. We use the NearestNeighbors³ API provided in SciKit-Learn in this experiment.

F Architecture Details

In this study, we use a slightly modified version of R(2+1)D-18 (Tran et al. 2018) as the video backbone as proposed in (Morgado, Vasconcelos, and Misra 2021), and ResNet-18 (He et al. 2016) as the audio backbone. For the sake of completeness, we present the architecture details in Tables S5 and S6, respectively. The predictor and projector heads are made of fully-connected layers following (Chen and He 2021), and their architecture details are presented in Table S7.

G Hyperparameters and Training Details

In this section, we present the details of the hyperparameters, computation requirements, as well as additional training details of self-supervised pretraining and full finetuning.

G.1 Pretraining Details

We present the pretraining hyperparameters of CrissCross in Table S10. Most of the parameters remain the same across all 3 datasets, with the exception of a few hyperparameters such as learning rates and epoch size which are set depending on the size of the datasets. We train on Kinetics-Sound with a batch size of 512, on a single node with 4 Nvidia RTX-6000 GPUs. Next, when training on Kinetics400 and AudioSet, we use 2 nodes and set the batch size to 2048. Adam (Kingma and Ba 2015) optimizer is used to train our proposed framework. We use LARC⁴(You, Gitman, and

³sklearn.neighbors.NearestNeighbors

⁴<https://github.com/NVIDIA/apex/blob/master/apex/parallel/LARC.py>

Layer	X_f	X_t	C	K_s	K_t	S_f	S_t
spectrogram	80	200	1	-	-	-	-
conv1	40	100	64	7	7	2	2
maxpool	20	50	64	3	3	2	2
block2.1.1	20	50	64	3	3	2	2
block2.1.2	20	50	64	3	3	2	2
block2.2.1	20	50	64	3	3	2	2
block2.2.2	20	50	64	3	3	2	2
block3.1.1	10	25	128	3	3	2	2
block3.1.2	10	25	128	3	3	2	2
block3.2.1	10	25	128	3	3	2	2
block3.2.2	10	25	128	3	3	2	2
block4.1.1	5	13	256	3	3	2	2
block4.1.2	5	13	256	3	3	2	2
block4.2.1	5	13	256	3	3	2	2
block4.2.2	5	13	256	3	3	2	2
block5.1.1	3	7	512	3	3	2	2
block5.1.2	3	7	512	3	3	2	2
block5.2.1	3	7	512	3	3	2	2
block5.2.2	3	7	512	3	3	2	2
avg-pool	-	-	512	-	-	-	-

Table S6: Architecture of the audio backbone: ResNet-18.

Layer	Dimensions
input	512
fc-bn-relu	2048
fc-bn-relu	2048
fc-bn	2048

Table S7: Architecture of projector heads.

Layer	Dimensions
input	2048
fc-bn-relu	512
fc	2048

Table S8: Architecture of predictor heads.

Ginsburg 2017) as a wrapper to the Adam optimizer to clip the gradients while pretraining with a batch size of 2048. In this work, we stick to batch sizes of 512 and 2048, because (i) as they show stable performance based on the findings of (Chen and He 2021); (ii) they fit well with our available GPU setups. Additionally, we perform mixed-precision training (Micikevicius et al. 2018) using PyTorch AMP (Paszke et al. 2019) to reduce the computation overhead.

Ablation Parameters. In the ablation study, we keep the training setup exactly identical across all the variants, with the exception of the learning rates, which we tune to find the best performance for that particular variant. For example, we set the base learning rate for \mathcal{L}_{v1v2} and \mathcal{L}_{a1a2} models as 0.0001 and 0.00001 respectively. Next, the predictor learning rates are set to 0.001 and 0.0001 for the \mathcal{L}_{v1v2} and \mathcal{L}_{a1a2} variants.

G.2 Full Finetuning Details

The full fine-tuning hyperparameters for both benchmarks are presented in Table S11. We use a batch size of 32 for the 32-frame input and 64 for the 8-frame input. We use an SGD optimizer with a multi-step learning rate scheduler to finetune the video backbones. Please note that we perform the full finetuning on a single Nvidia RTX-6000 GPU.

H Limitations.

The notion of asynchronous cross-modal optimization has not been explored beyond audio-visual modalities. For example, our model can be expanded to consider more than 2 modalities (e.g., audio, visual, and text), which are yet to be studied. Additionally, we notice a considerable performance gap between full-supervision and self-supervision when both methods are pretrained with the same large-scale dataset (Kinetics400 or AudioSet), showing room for further improvement.

I Broader Impact.

Better self-supervised audio-visual learning can be used for detection of harmful contents on the Internet. Additionally, such methods can be used to develop better multimedia systems. Lastly, the notion that relaxed cross-modal temporal synchronicity is useful, can challenge our existing/standard approaches in learning multi-modal representations and result in new directions of inquiry. The authors don't foresee any major negative impacts.

Abbreviations	Name	Description
bs	batch size	The size of a mini-batch.
es	epoch size	The total number of samples per epoch.
ep	total epochs	The total number of epochs.
lr	learning rate	The learning rates to train the networks.
lr _{ab}	audio backbone lr	
lr _{vb}	video backbone lr	
lr _{ap}	audio predictor lr	
lr _{vp}	video predictor lr	
lrs	learning rate scheduler	The learning rate scheduler to train the network.
ms	milestones	At every ms epoch the learning rate is decayed.
γ	lr decay rate	The learning rate is decayed by a factor of γ .
wd	weight decay	The weight decay used in the SGD optimizer.
mtm	momentum	The momentum used in the SGD optimizer.
drp	dropout	The dropout rate.

Table S9: Abbreviations and descriptions of the hyperparameters.

dataset	bs	es	ep	optim	lrs	lr _{vb} (start/end)	lr _{ab} (start/end)	lr _{vp}	lr _{ap}	wd	betas
KS	512	220K	100	Adam	Cosine	0.0002/0	0.0002/0	0.002	0.002	0.0001	0.9, 0.999
K400	2048	1M	100	Adam*	Cosine	0.0002/0.0001	0.0002/0.0001	0.002	0.002	0.0001	0.9, 0.999
AS	2048	3.5M	100	Adam*	Cosine	0.0001/0	0.0001/0	0.001	0.001	0.0001	0.9, 0.999

Table S10: Pretext training parameters. Note the abbreviations used below, KS: Kinetics-Sound, K400: Kinetics400, AS: AudioSet, Adam*: Adam with LARC

dataset	input	es	bs	ep	ms	optim	lrs	lr	γ	wd	mtm	drp
UCF101	8×224^2	95K	64	20	6/10/14	SGD	multi-step	0.0005	0.3	0.0	0.9	0.0
UCF101	32×224^2	95K	32	20	8/12/16	SGD	multi-step	0.00007	0.3	0.0	0.9	0.0
HMDB51	8×224^2	35K	64	20	6/10/14	SGD	multi-step	0.0005	0.1	0.0	0.9	0.0
HMDB51	32×224^2	35K	32	20	8/12/16	SGD	multi-step	0.0001	0.3	0.0	0.9	0.0

Table S11: Full-finetuning hyperparameters for action recognition when pretrained on Kinetics400.